Internal Charge Estimates for Satellites in Low Earth Orbit and Space Environment Attribution

Robert J. Redmon, Juan V. Rodriguez, Carl Gliniak, and William F. Denig

***Abstract*— Space assets are continuously bathed by charged particles making their components susceptible to the effects of spacecraft charging. While their orbits are not embedded within the radiation belts, low earth orbiting assets with high inclinations do pass through the horns of these belts during each polar crossing, transiting through potentially dangerous charged particle populations many times per day. Occasionally, these low altitude horns include significant populations of energetic ∼1 MeV electrons, which can penetrate typical spacecraft shielding and accumulate within dielectric materials and on ungrounded conductors, a process known as internal charging. The National Oceanic and Atmospheric Administration Polar Operational Environmental Satellites (POES) have experienced on-orbit anomalies in the boost voltage regulator (BVR) that is suspected to be associated with the accumulation and discharge of ∼800 keV electrons. We have used observations from the Medium Energy Proton and Electron Detector (MEPED) instrument and a first principles model of charge accumulation [11] to develop estimates of electron internal charge (IC) accumulation over the lifetime of each POES and Metop spacecraft for a range of typical discharge time constants. With the advantage afforded by a larger database of anomalies, we are able to show that these BVR anomalies are generally not attributable in a simple way to the accumulation and subsequent discharge from >800 keV nor a higher fluence of lower energy >300 keV electrons. To the best of our knowledge, this paper presents the first long-term estimates of IC for spacecraft in highly inclined low earth orbits.**

***Index Terms*— Electrostatic discharges, low earth orbit satellites, plasma measurements, radiation effects, space radiation.**

I. Introduction

OF THE hazards encountered by modern spacecraft, anomalies directly attributable to interactions with charged particles cover the range from recoverable to catastrophic failure of important systems [26], [27]; however, such space environmental effects are believed to be a minor, roughly 26%, subset of the issues experienced [39]. Environmental impacts to spacecraft include electrostatic discharge (ESD) from an accumulation of electrons (keV to MeV) on surface and internal components [11], [28]–[32], single event effects (SEE) due to energetic heavy ions (MeV to GeV) [33], [34] and degradation due to total ionizing dose (TID) [35]. While spacecraft subsystems are designed to shunt charges away from susceptible components, if the electric potential from charge accumulation exceeds the breakdown voltage then an internal ESD (IESD) occurs, which can cause soft anomalies and permanent damage. This paper is focused on assessing the likelihood of IESD attribution of a particular history of power system anomalies experienced by the U.S. National Oceanic and Atmospheric Administration (NOAA) Polar Operational Environmental Satellites (POES) program assets.

Manuscript received July 28, 2016; accepted September 26, 2016. Date of publication May 17, 2017; date of current version August 9, 2017. *(Corresponding author: Robert J. Redmon.)*

R. J. Redmon and W. F. Denig are with the NOAA National Centers for Environmental Information, Boulder, CO 80305 USA (e-mail: rob.redmon@noaa.gov; william.denig@noaa.gov).

J. V. Rodriguez is with the Cooperative Institute for Research in Environmental Sciences, University of Colorado Boulder, Boulder, CO 80309 USA, and also with the NOAA National Centers for Environmental Information, Boulder, CO 80305 USA (e-mail: juan.rodriguez@noaa.gov).

C. Gliniak is with the NOAA National Environmental Satellite, Data, and Information Service, Office of Satellite and Product Operations, Suitland, MD 20746 USA (e-mail: carl.gliniak@noaa.gov).

Color versions of one or more of the figures in this paper are available online at http://ieeexplore.ieee.org.

Digital Object Identifier 10.1109/TPS.2017.2656465

II. Anomaly History

The NOAA and the European Organisation for the Exploitation of Meteorological Satellites (EUMETSAT), respectively, operate the POES and the meteorological operational (Metop) satellites. These spacecraft are in a fixed local time, retrograde, low earth orbit (LEO) with periods of roughly 102 minutes and altitudes of approximately 850 km. At the time of this paper, the program includes five operational spacecraft identified as: NOAA-15, -18, -19, Metop-A, and Metop-B. A diverse suite of instrumentation is manifested including the Space Environment Monitor (SEM-2).

Powering the spacecraft is accomplished by the solar array when sunlit and by batteries when in darkness and anytime the solar array output is insufficient. Within the electrical power subsystem power supply electronics, it is the boost voltage regulator (BVR) through which supplemental battery power flows [1], [15]. NOAA-16, -17, and -18 were launched on September 21, 2000, June 24, 2002, and May 20, 2005, respectively. Between their placement into operations and the time of this paper, BVR phase controllers on these spacecraft have autonomously switched to backup seven times [2], [3] (five events on NOAA-18), each time a nondetrimental but nevertheless anomalous and unpredicted event.

Table I summarizes the BVR anomalies to date with content sufficient to initiate anomaly investigations [4], [5]. The spacecraft geographic and magnetic coordinates (latitude, longitude, local time, and L-shell) for the minute nearest to the anomaly was calculated using the National Aeronautics and Space Administration (NASA) Space Physics Data Facility (SPDF) Locator application. The longitudes provided are positive eastward. Table II summarizes the space environment leading up to and during each anomaly. Column 3 indicates the level of geomagnetic activity at the anomaly time using two

TABLE I
HISTORY OF BVR ANOMALIES ON NOAA-16, NOAA-17 AND NOAA-18 SPACECRAFT

#	Event Time (UTC)	S/C	Geographic[*1]			Magnetic[*1]			
			Lat	Lon	LT	Lat	Lon	LT	L
1	2006-03-29 05:02:32	N18	-32.1	136.6	14:09	-40.9	212.3	14:20	1.9
2	2007-01-04 09:32:15	N18	69.8	37.1	12:00	64.7	130.2	13:38	6.1
3	2007-07-19 18:58:43	N16	75.2	279.0	13:35	84.9	333.4	12:28	N/A[*2]
4	2007-09-17 08:04:51	N17	-54.8	17.9	09:16	-53.6	76.0	08:27	3.1
5	2011-03-08 21:55:00	N18	-64.0	44.9	00:55	-66.9	96.0	23:17	7.4
6	2013-01-21 16:32:00	N18	-42.3	150.4	02:34	-49.2	230.1	02:53	2.6
7	2015-01-22 08:51:24	N18	-65.8	276.3	03:16	-56.0	351.6	03:31	3.6

[*1]Used nearest minute to the anomaly time. Calculation is from NASA SPDF Locator.
[*2]Magnetic latitude was too high to calculate a meaningful L-value.

TABLE II
SPACE ENVIRONMENT DURING ANOMALIES

#	Event Time (UTC)	Geomagnetic Activity (Time of Anomaly)	Geomagnetic Activity (Worst Previous 5 Days)	SEP Event
1	2006-03-29 05:02:32	Quiet Kp: 2, Dst: -11nT	Moderate Kp: 3.3, Dst: -29nT	No
2	2007-01-04 09:32:15	Moderate Kp: 3.3, Dst: -21nT	Moderate Kp: 4.7, Dst: -30nT	No
3	2007-07-19 18:58:43	Quiet Kp: 0.3, Dst: 3nT	Active Kp:5.3, Dst: -45nT	No
4	2007-09-17 08:04:51	Quiet Kp: 0, Dst: 4nT	Quiet Kp: 2.3, Dst: +28nT	No
5	2011-03-08 21:55:00	Quiet Kp: 1.3, Dst: -13nT	Moderate Kp: 3.7, Dst: -27nT	Yes
6	2013-01-21 16:32:00	Quiet Kp: 0.7, Dst: -8nT	Moderate Kp: 4, Dst: -53nT	No
7	2015-01-22 08:51:24	Quiet Kp: 2.3, Dst: -7nT	Moderate Kp: 3.7, Dst: +45nT	No

regularly used measures, the roughly midlatitude Kp [23] and low-latitude disturbance storm-time (D_{st}) [24] activity indices and these classifications using Kp: Quiet is [0,3), Moderate is [3,5), and Active is $Kp \geq 5$. Column 4 is the same as column 3 for the worst case within the previous five days. Column 5 indicates whether or not a solar energetic particle (SEP) event is in progress using observations of >10 MeV protons (p^+/cm^2-sr-sec) from the NOAA Geostationary Operational Environmental Satellite Energetic Proton, Electron, and Alpha Detector with an SEP event threshold of >10 p^+/cm^2-sr-sec. From Tables I and II, we draw a few key points. The anomalies are not clearly organized by location or global environmental

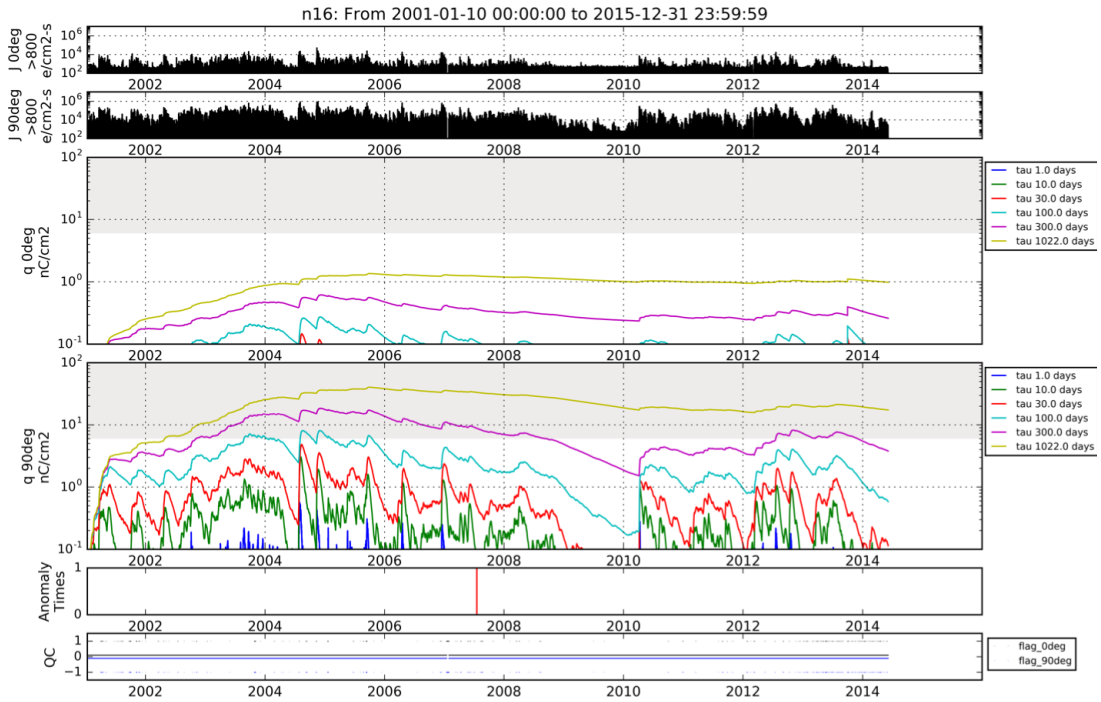

Fig. 1. NOAA-16 observed outer radiation belt >800 keV electron number fluxes and estimated accumulated charge. Panels from top to bottom are: (a) and (b) flux (e-/cm^2-sec) observed by the zenith (0°) and antivelocity (90°) telescopes, (c) and (d) accumulated charge estimates (nC/cm^2) from the zenith and antivelocity telescopes for the time constants 1 (blue), 10 (green), 30 (red), 100 (cyan), 300 (magenta), and 1022 (yellow) days, (e) anomaly times, and (f) quality flags. The gray shading in panels (c) and (d) indicate charge densities exceeding 6 nC/cm^2. The quality flags in panel (f) (zenith detector is black, antivelocity detector is blue) are set to +1 (zenith) or −1 (antivelocity) when valid flux data did not exist. For all panels, the time range shown is from 2001-01-10 to 2015-12-31.

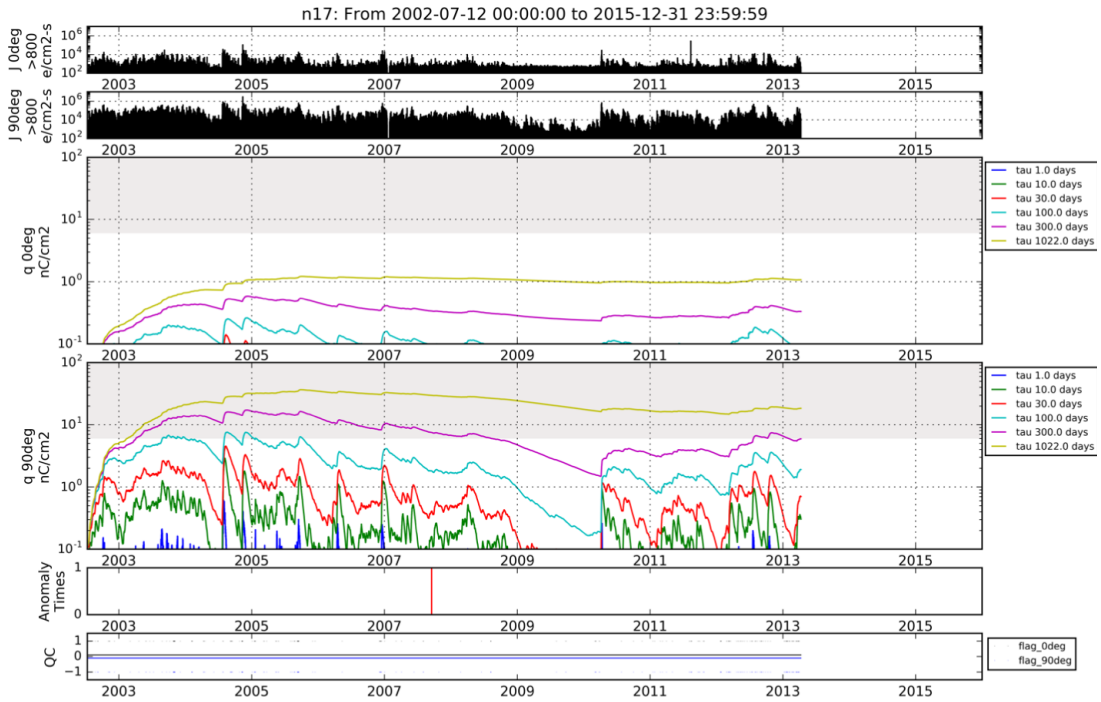

Fig. 2. NOAA-17; the same format as Fig. 1. For all panels, the time range shown is from 2002-07-12 to 2015-12-31.

activity. Anomalies occurred both outside and within the outer electron radiation belt ($L \sim 3$–8), none occurred in the South Atlantic Anomaly, some were in sunlight, all occurred during quiet to moderate levels of geomagnetic activity and one occurred, while an SEP event was in progress.

Earlier (unpublished) analyses of the first four of these anomalies suggested internal charge (IC) accumulation from >800 keV electrons and subsequent IESD as a likely cause. In Section III, we develop mission lifetime IC estimates and evaluate their correlation with BVR anomalies in Section IV.

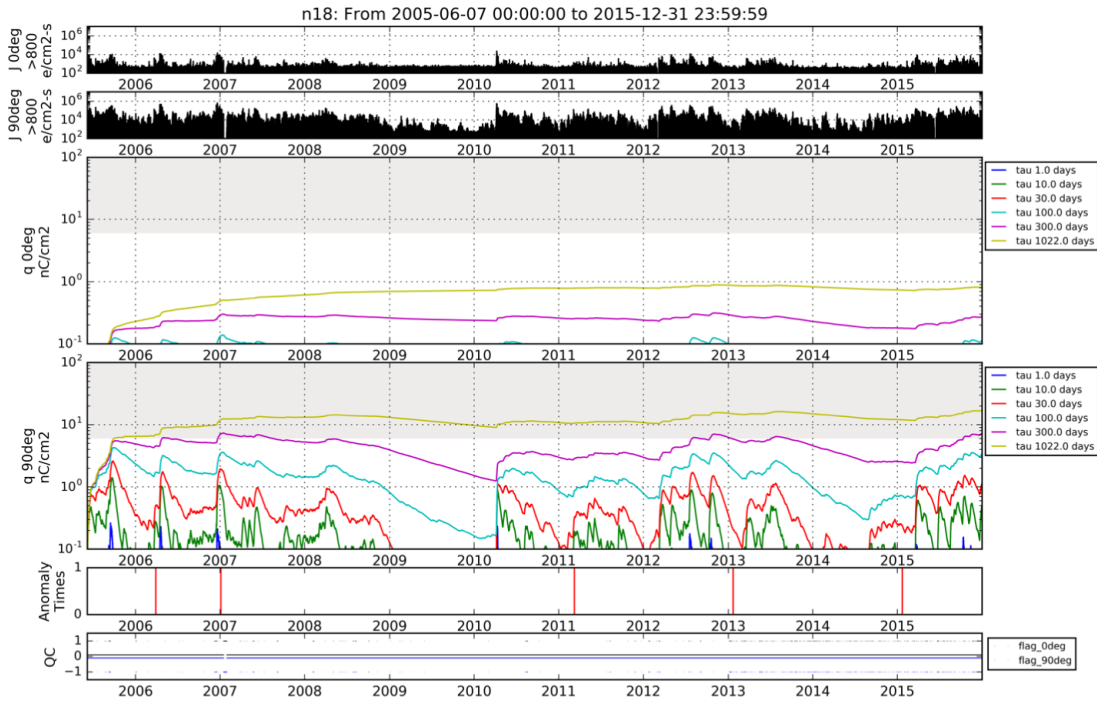

Fig. 3. NOAA-18; the same format as Fig. 1. For all panels, the time range shown is from 2005-06-07 to 2015-12-31.

III. *In Situ* Space Particle Observations

A. Instrumentation

POES and Metop spacecraft are all equipped with a SEM-2 instrument suite, which includes the total energy detector (TED), and medium energy proton and electron detector (MEPED).

The TED instrument measures the flux of electrons and ions in the energy range of 0.05–20 keV from two look directions (zenith and 30° off zenith). The MEPED instrument consists of four telescopes for measuring electron and proton particle fluxes in two look directions that are nominally zenith (0°) and antivelocity (90°) and four omnidirectional dome detectors ("omnis") for measuring proton particle fluxes. Compared to Metop, the POES spacecraft MEPED instrument is rotated off axis in two planes by approximately 9° each (see [8], their Figs. 2–5).

In 2012, processing of the POES/Metop SEM-2 observations transferred from the US NOAA National Weather Service Space Weather Prediction Center (SWPC) to the NOAA National Centers for Environmental Information (NCEI) and for approximately three years, SEM observations were processed by both organizations. During this transition processing was changed from the description in [9] to [7] and [8]. Most notably, with respect to MEPED, charged particle measurements reported in 16-second averaged count rates before 2012 are now reported as calibrated number fluxes at a 2-second cadence. Now, electron telescope particle fluxes are reported for integral ranges with minimum energies of 40, 130, 287, and 612 keV. The pseudonyms for these ranges are E1, E2, E3, and E4. Proton telescope particle fluxes are now reported at five differential energies of 39, 115, 332, 1105, and 2723 keV and for one integral range of $>$6423 keV. Their pseudonyms are P1–P6. Omnidirectional proton fluxes derived from the omnis are now reported at three differential energies of 25, 50, and 100 MeV. The availability and processing of the standard POES/Metop SEM-2 measurements are collectively described in [6]–[9] and [36].

The highest energy directional electron channel, E4, is derived from the highest energy proton channel, P6, which is particularly responsive to electrons that are $>$612 keV, a beneficial use of otherwise cross-species contamination [8], [10]. P6 is used as E4 whenever high energy protons are not present (e.g., such as during SEP events). Being immune to cross-species contamination [10], a P5 count rate of $<$3 counts/s is used for that determination [8].

Based on Geant4 simulations [21], [22], the electron response function (cm^2 sr) of E4 turns on around 400 keV and increases slowly with energy (two orders of magnitude between 400 and 2000 keV) [10]. The effective lower energy of such channels is ambiguous without knowledge of the electron energy spectrum being measured. Since electron spectra are usually steep in this energy range, the effective energy is much less than the energy at which the electron response function is maximum. Bowtie analysis [16], [17] uses a representative family of particle spectra to estimate the effective energy at which the spread in geometric factors due to natural variability is minimized. The bowtie analyses used to derive the MEPED telescope geometric factors used in the NCEI processing [8] followed this approach. For the accumulated charge assessment from the E3 channel (nominally $>$300 keV), we use the geometric factor of 0.0075 cm^2 sr at $>$287 keV effective energy derived by [8]. The same analysis resulted in an E4 geometric factor of 0.0055 cm^2 sr

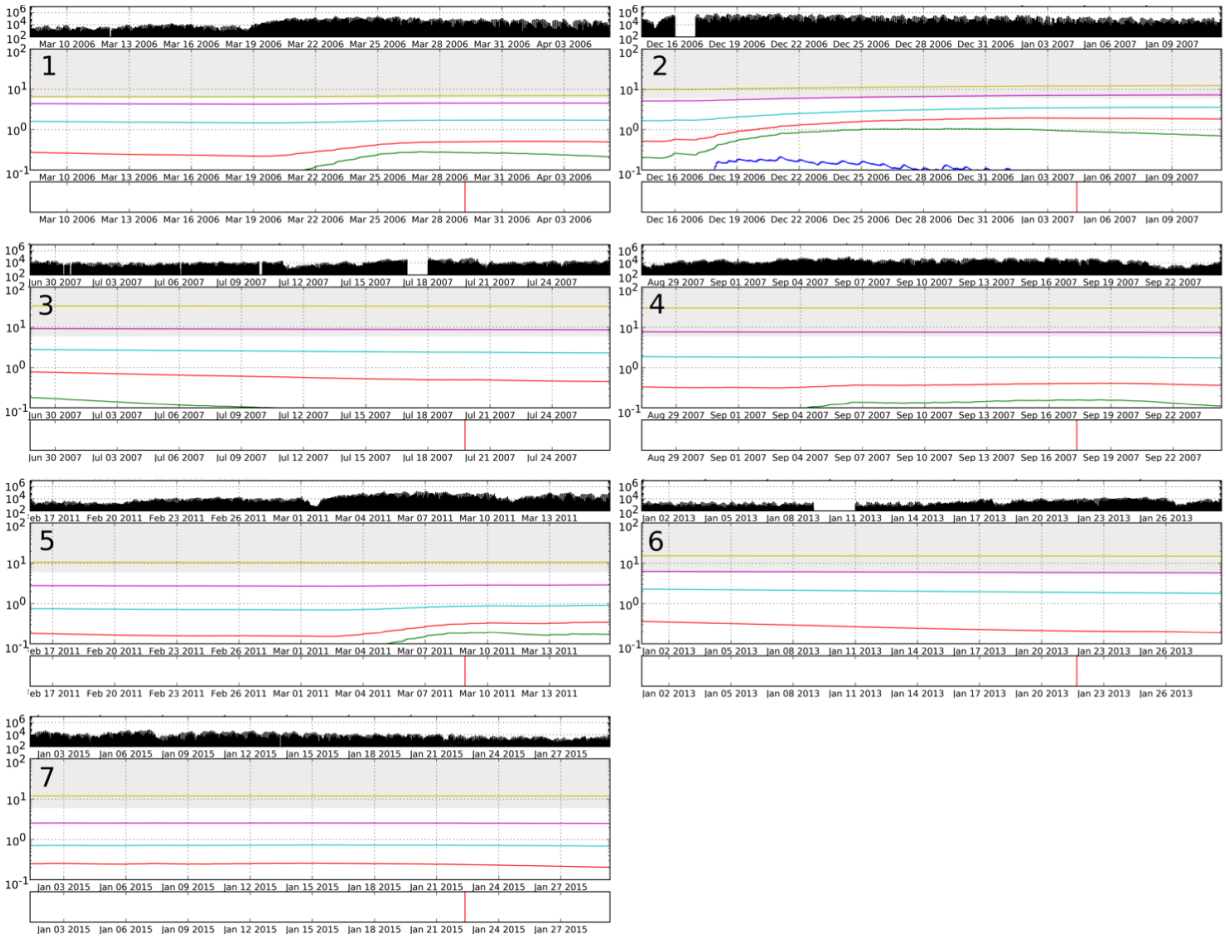

Fig. 4. Anomaly events one to seven (Table I) for the time range of 21 days before the anomaly to seven days afterward. For each of the seven numbered panels/events, the layout from top to bottom is: (a) flux (e-/cm^2 sec) observed by the antivelocity (90°) telescope, (b) accumulated charge estimate (nC/cm^2) from the antivelocity telescope for the time constants 1 (blue), 10 (green), 30 (red), 100 (cyan), 300 (magenta), and 1022 (yellow) days, and (c) anomaly time. The gray shading in each (b) indicates charge density exceeding 6 nC/cm^2. Flux gaps indicate times when observations were not available. For the gap in event 3, using N17 as a proxy for N16's gap does not change the IC curves substantially. For all panels, the total time range shown is 28 days.

for >612 keV, which is significantly less than the >800 keV assumed for this channel in the present anomaly investigation.

Since we are assessing the attribution potential of >800 keV electron accumulation to the BVR anomalies, we are effectively estimating the charge available to accumulate on dielectrics that are behind shielding equivalent to ~60 mil (1524 μm) of aluminum, midway between 42 mil (1072 μm) at 600 keV and 81 mil (2054 μm) at 1000 keV, the latter of which is more typical of spacecraft shielding (from [11], their Fig. 10). By fixing the E4 effective lower energy at 800 keV, a bowtie analysis was used to compute a new geometric factor [0.0064 cm^2 sr (+10.3% upper quartile and −9.2% lower quartile)] for estimating the flux of >800 keV electrons from the E4 channel. The larger geometric factor is consistent with smaller fluxes expected at 800 than at 612 keV. For consistency within this anomaly resolution study, we maintain the E4 effective energy at 800 keV and use the new geometric factor.

Finally, the NCEI data (≥2013) are smoothed with a seven-point moving average filter for merging with the SWPC (<2013) 16-second averages. We use these updated MEPED measurements for our IC estimates developed in the next section.

B. Internal Charge Estimates

The accumulation of incident >800 keV electrons followed by an IESD was suspected by the POES program as a potential cause of the BVR anomalies. In this section, we develop IC estimates from SEM-2 observations to test for a correlation between IC accumulation and anomaly times. The first principles 1-D charge accumulation model of [11] was adapted to estimate IC accumulation for the mission lifetimes of all POES/Metop spacecraft for various dielectric material charge dissipation time constants. This method has been used in other studies for satellites in a Medium Earth Orbit (MEO), Highly Elliptical Orbit (HEO), or Geostationary Equatorial Orbit (GEO) [11], [12] and recently, for the elliptical, low inclination orbit of the Van Allen Probes [13]. To the best of our knowledge, this paper presents the first long-term estimates for highly inclined LEO assets.

A summary of the method as applied to POES/Metop follows. The integration time step is 16-seconds (compared to one day in [11]). For each time step, since mission start, the charge density is accumulated and decayed (adapted

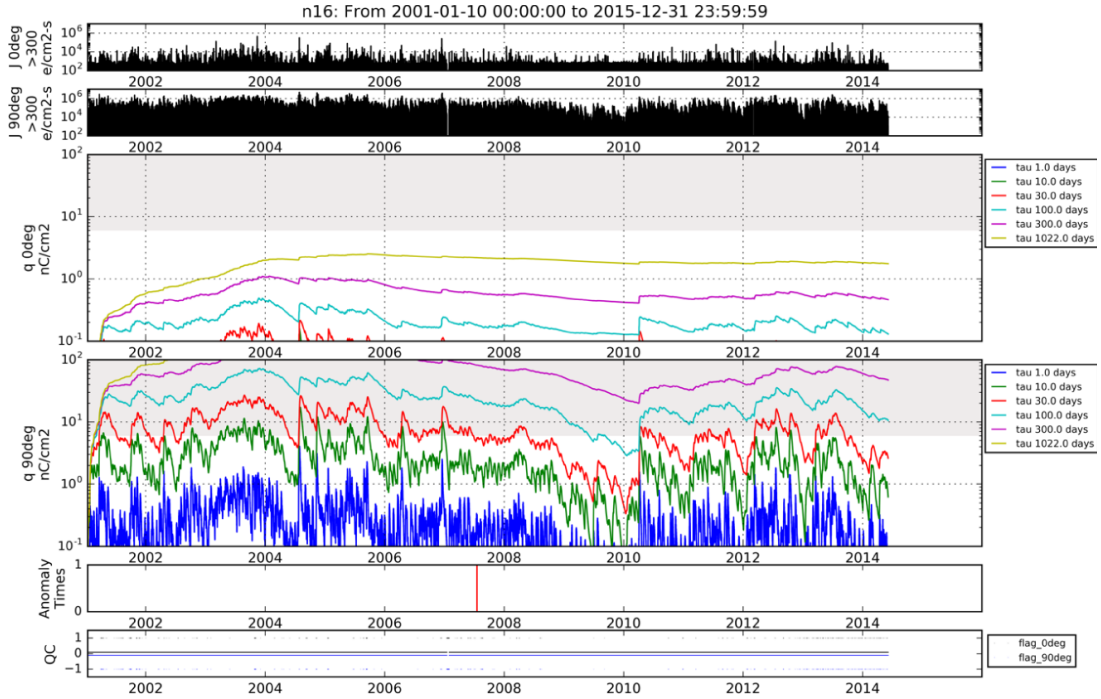

Fig. 5. NOAA-16, electrons >300 keV; the same format as Fig. 1.

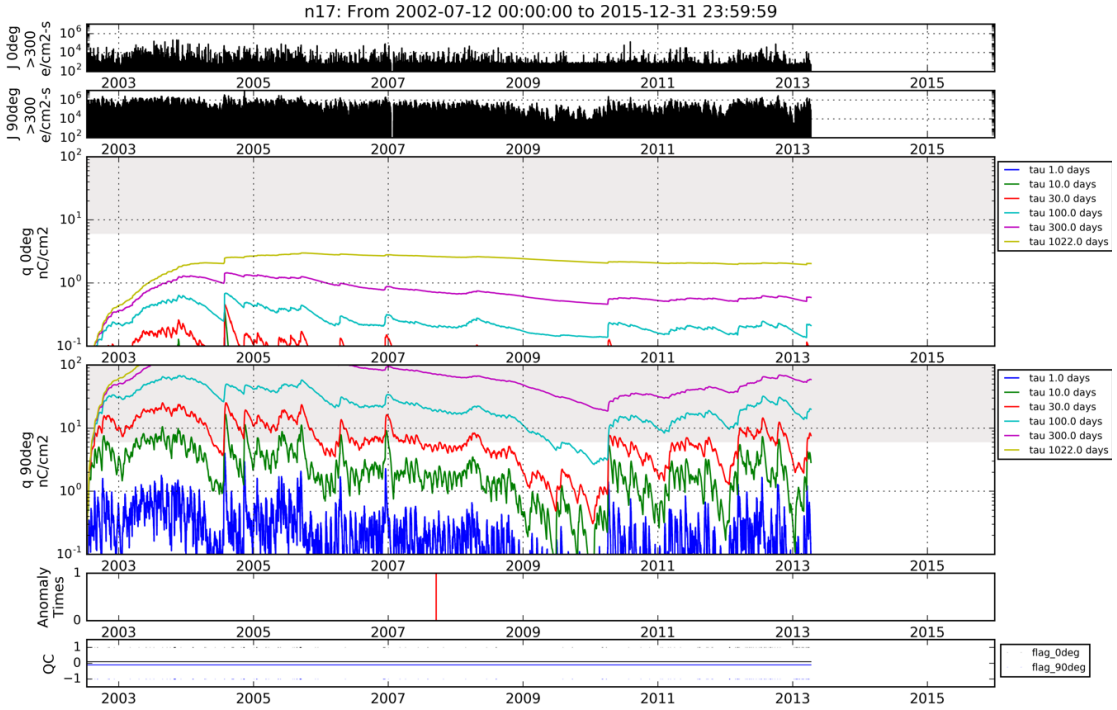

Fig. 6. NOAA-17, electrons >300 keV; the same format as Fig. 1.

from [11])

$$\alpha = e^{-\Delta t/\tau}$$
$$q_n = \alpha \cdot q_{n-1} + \tau(1-\alpha)(J_n \cdot 1.6 \times 10^{-10} nC). \quad (1)$$

Here, q_n and J_n are the charge density (nC/cm^2) and incident electron number flux (e$^-$/cm^{2}s) at time step n, Δt is 16-seconds, and τ is the dielectric material charge decay time constant (seconds). The initial conditions J_0 and q_0 are assumed to be 0. The number flux J_n in (1) is acquired as follows. We assume J_n is 0 unless the spacecraft is within a magnetic McIlwain L-shell [14] range of 3–8 (typical outer radiation belt range) to ensure we are observing outer radiation belt electrons rather than inner belt protons or SEPs. As described previously, P5 serves as an additional filter for proton contamination of the >800 keV electron fluxes. After application of the appropriate geometric factor, the fluxes described in Section III-A are in units of directional

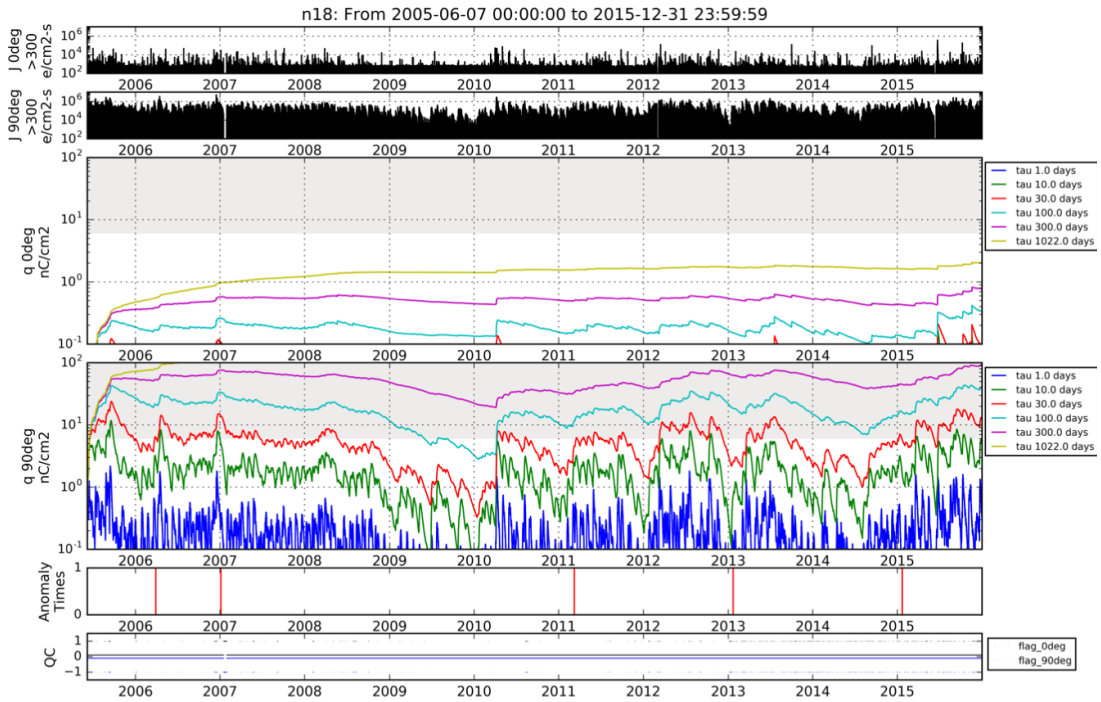

Fig. 7. NOAA-18, electrons >300 keV; the same format as Fig. 1.

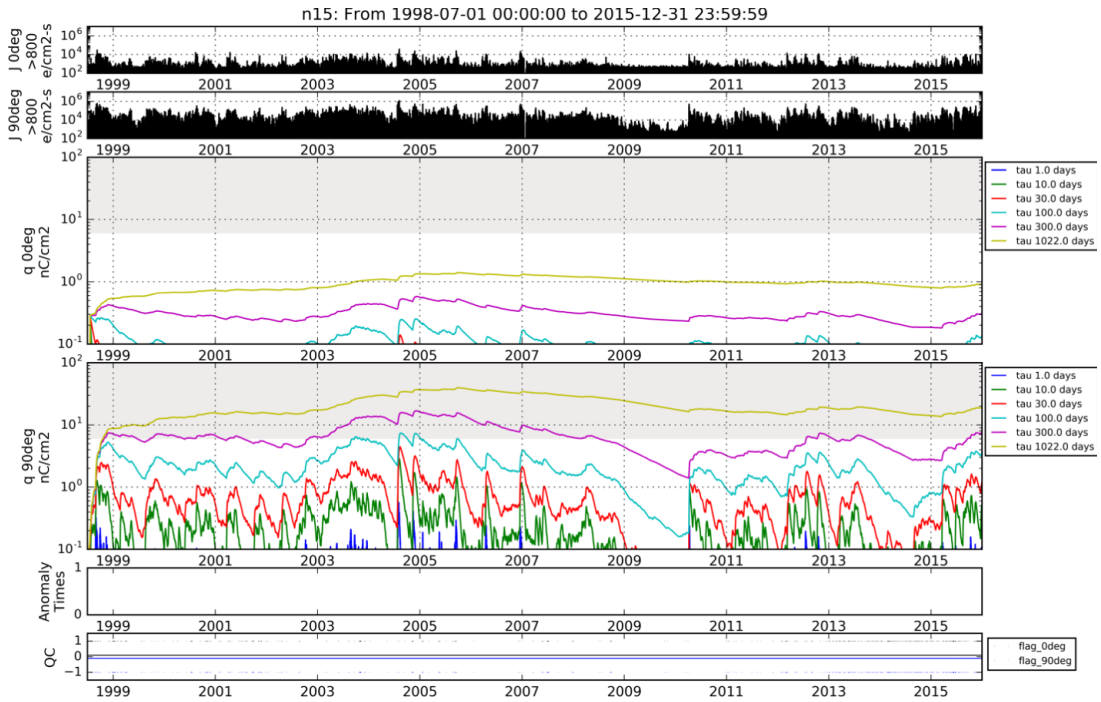

Fig. 8. NOAA-15, electrons >800 keV; the same format as Fig. 1.

number flux (e^-/cm^2-sr-sec). We estimate the flux projected onto a planar surface by assuming isotropy over the detector field of view and thus simply by multiplying the fluxes in Section III-A by π. With this algorithm, the charge density q_n is separately calculated for the zenith and antivelocity MEPED detector look directions, the electron energy ranges of >300 and >800 keV and six time constants, resulting in 24 charge density time series per spacecraft.

The mission lifetime fluxes of >800 and >300 keV electrons and their estimated IC accumulation for NOAA-16, -17, and -18 are shown in Figs. 1–3 and 5–7, respectively. Similar calculations were computed for POES/Metop satellites not experiencing BVR anomalies (see Figs. 8–15). Preliminary estimates for NOAA-18 were presented and discussed at the 14th Spacecraft Charging Technology Conference held in Noordwijk, NL [40]. The IC accumulation has been

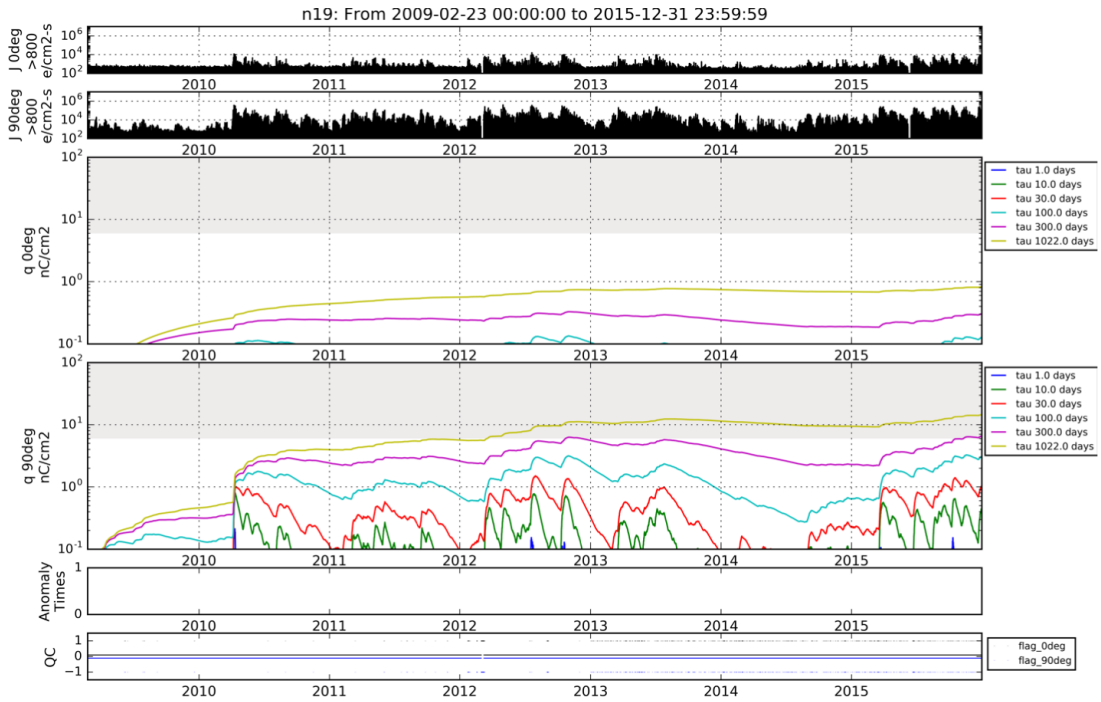

Fig. 9. NOAA-19, electrons >800 keV; the same format as Fig. 1.

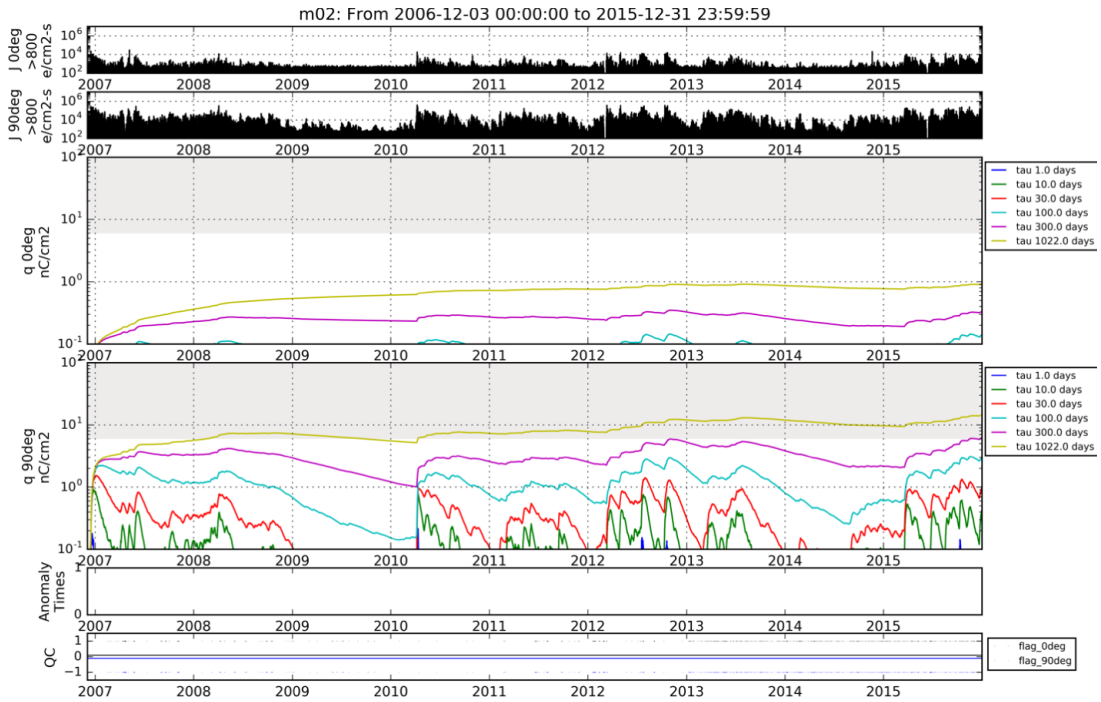

Fig. 10. Metop-A, electrons >800 keV; the same format as Fig. 1.

calculated for six time constants (τ days): 1, 10, 30, 100, 300, and 1022 (~2.8 years). For the purpose of evaluating the association between IC accumulation and BVR anomaly times, we present a zoomed-in view for each event in Fig. 4. A critical charge density threshold of 6–20 nC/cm^2 captures most materials in space (see [11] and references therein). Therefore, charge densities >6 nC/cm^2 in all such figures are shaded with a gray background. Since only larger values of τ result in charge densities exceeding this threshold, using 24-hour averaged fluxes in (1) would be more computationally efficient (such as in [11]). We evaluate the merits of IC/IESD attribution in Section IV.

IV. Results and Discussion

Here, we discuss the essential features of the new IC estimates and the potential causality between the BVR

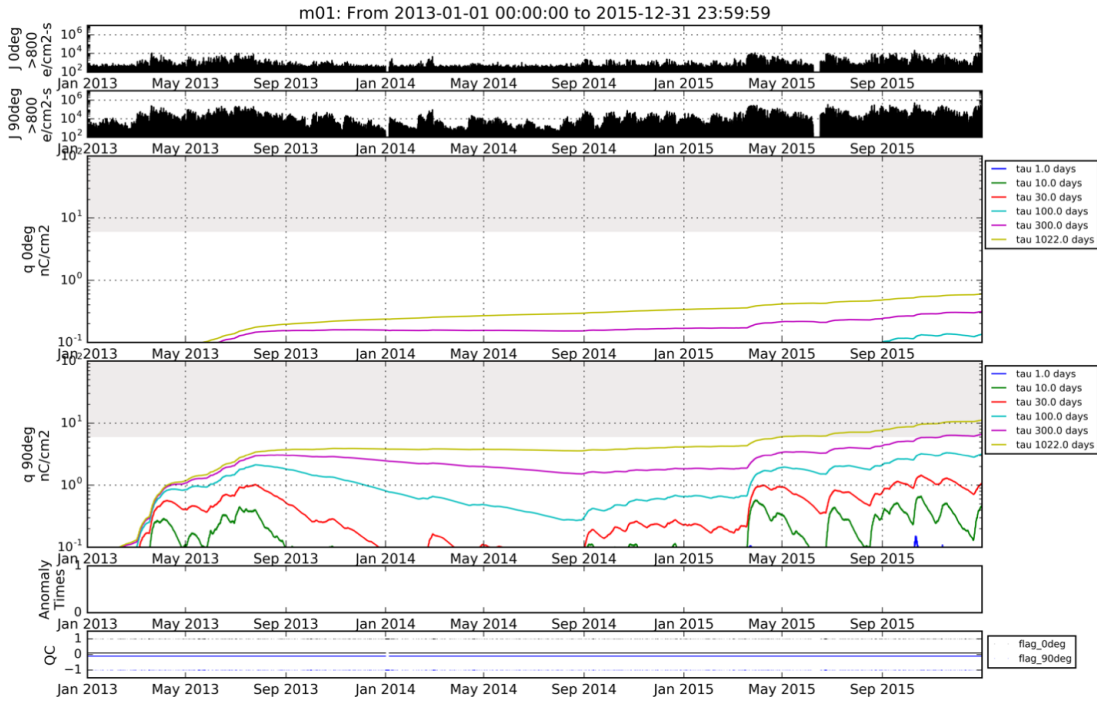

Fig. 11. Metop-B, electrons >800 keV; the same format as Fig. 1.

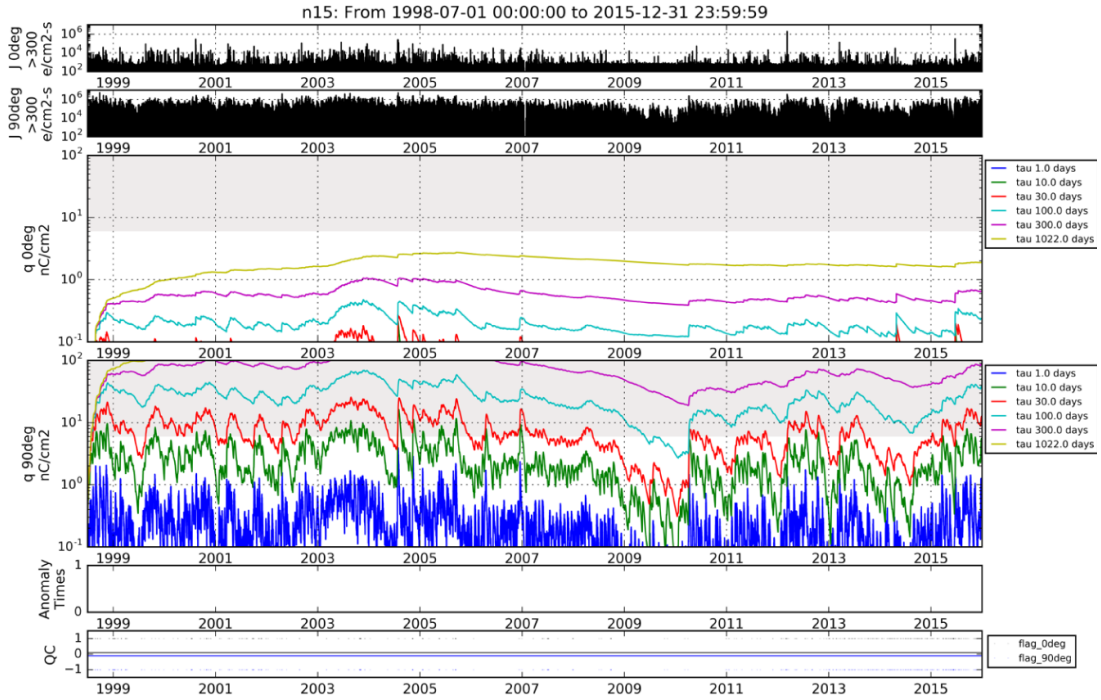

Fig. 12. NOAA-15, electrons >300 keV; the same format as Fig. 1.

anomaly events and IC/IESD. As predicted by (1), increases in IC accumulation occur abruptly for every τ, while charge dissipation takes time, more so for larger τ. From [11], the worst case GEO charging period was found to be 1994–1995 (before our observing period) and the second worst to be approximately 2004–2006 (with longer τ extending this range), which is in agreement with the worst case period in our study (e.g., our Fig. 8). There are many periods of elevated IC that are not temporally coincident with reported BVR anomalies [2], [3].

Reviewing Fig. 3, it is tempting to interpret a positive correlation between the first two BVR anomalies and peaks in the >800 keV IC accumulation estimates for NOAA-18. However, with a closer look near the time preceding each anomaly (as afforded in Fig. 4), the timing of BVR anomalies is not clearly linked to IC estimates across the seven events.

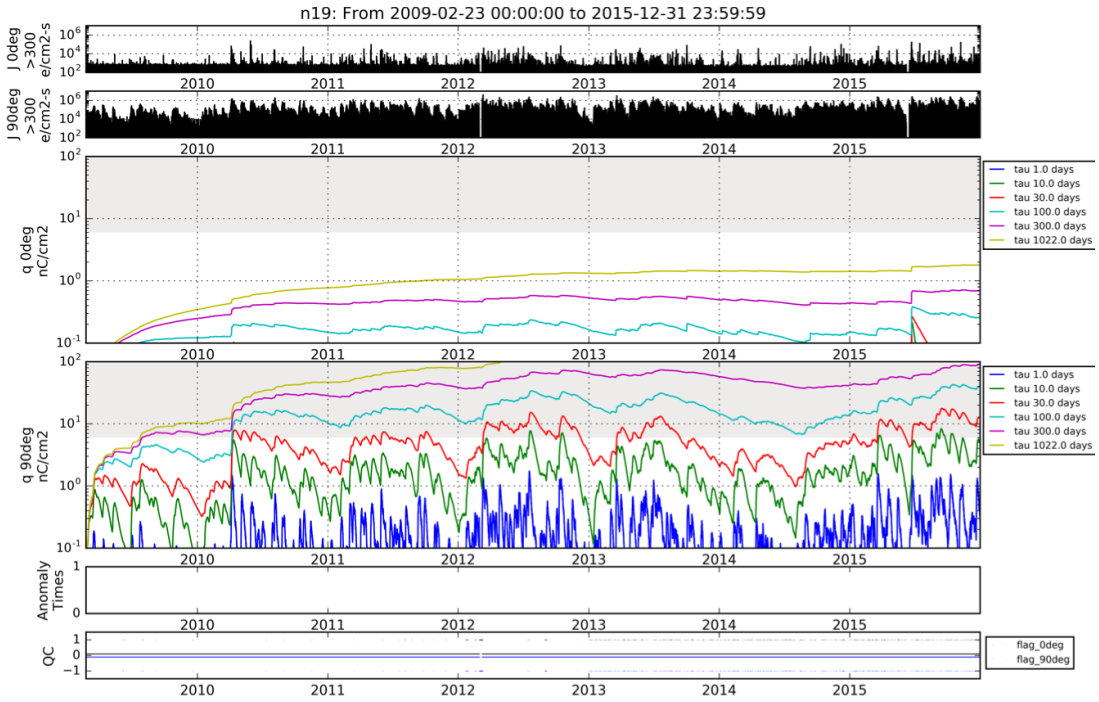

Fig. 13. NOAA-19, electrons >300 keV; the same format as Fig. 1.

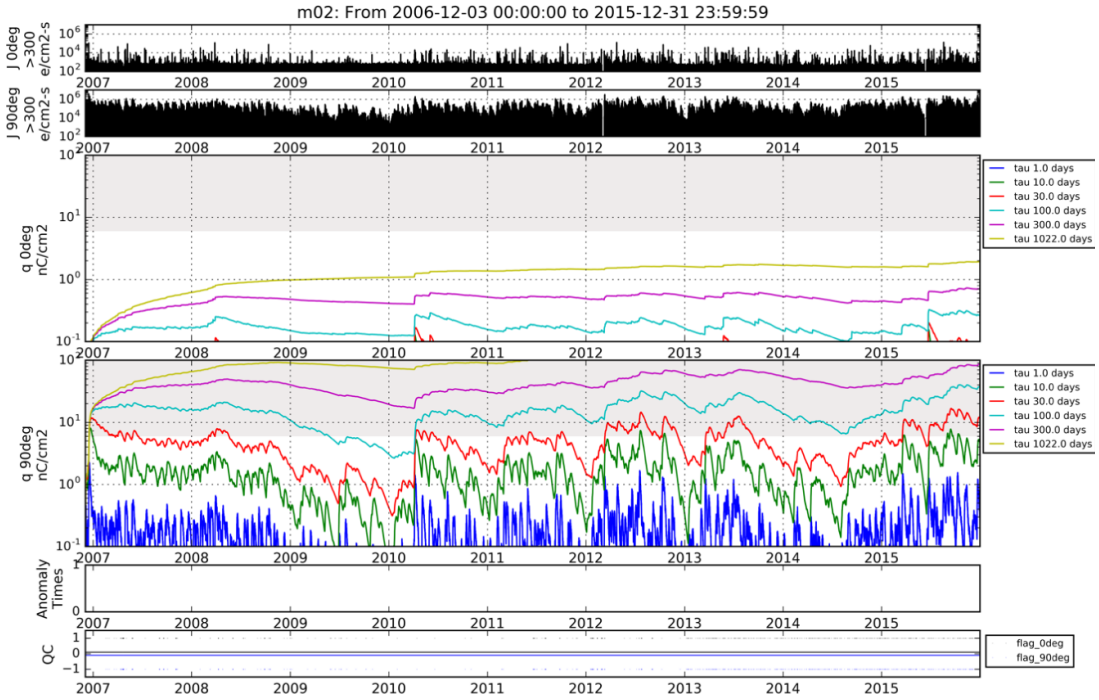

Fig. 14. Metop-A, electrons >300 keV; same format as Fig. 1.

Events one, two, and five show modest rises in IC for shorter τ (less resistive dielectrics), but no significant increases of the charge density occur near the lower threat level of 6 nC/cm^2 for any anomaly. A charge density of 6 nC/cm^2 (lower threat level) is only exceeded for τ of 2.8 years (all events), 300 days (events two to six), and no other time constants. For these larger τ (highly resistive dielectrics), the IC curves are resident in the >6 nC/cm^2 range for significant portions of the mission life, implying many more anomalies should have occurred if there was a direct IC link.

Lightly shielded or ungrounded cables exposed to the radiation environment are a classic source of anomalies in which excess accumulated charge in cable dielectrics leads to ESD, resulting in spurious signals [37], [38]. Cables can be particularly susceptible to charge accumulation due to their use of high-resistivity insulators [12]. While 1 MeV is required for electrons to penetrate 2 mm of aluminum, only 300 keV is required to penetrate 0.4 mm [11]. In 16 years of observations, the second-greatest levels of MEPED >300 keV electron fluxes on field lines that map

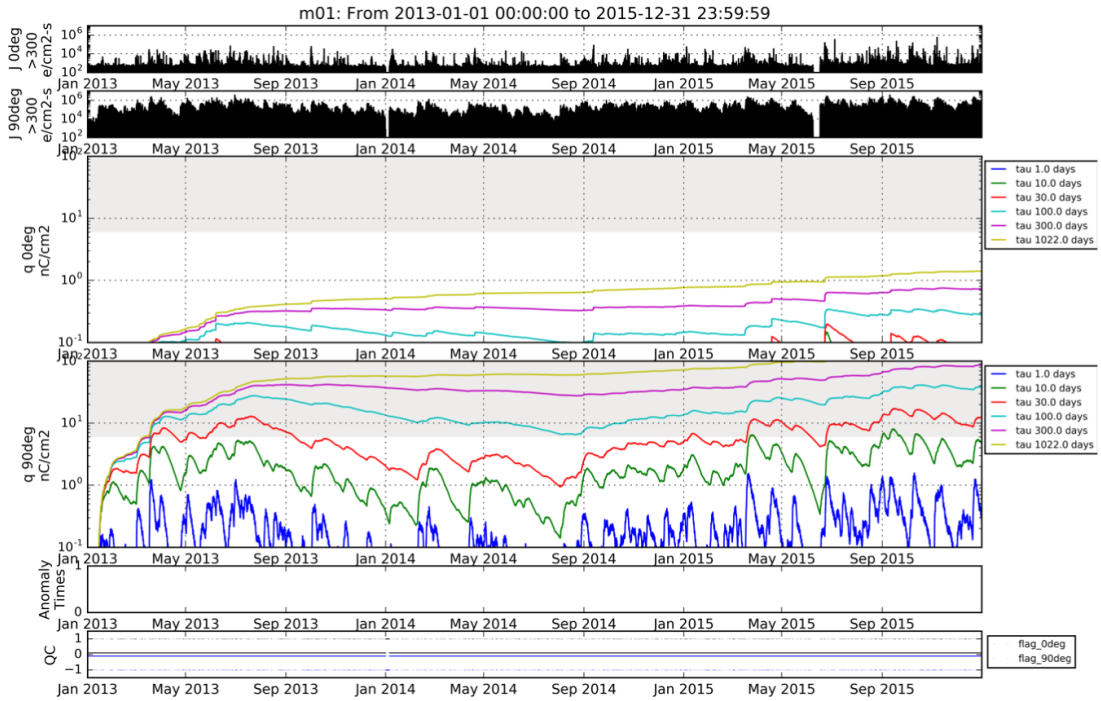

Fig. 15. Metop-B, electrons >300 keV; the same format as Fig. 1.

to geosynchronous orbit were observed at the time of the Galaxy-15 anomaly, corresponding to a 1-in-9.6 year event [25]–[27]. While this single observation of elevated radiation conditions at the time of an anomaly does not constitute proof of a causal relationship between the two, it suggests that charge accumulation due to >300 keV electrons should be evaluated in any internal charging investigation using MEPED data, in order to identify possible susceptibility to cable charging.

Figs. 5–7 present IC estimates for >300 keV electrons. In those estimates while the IC curves for every τ are elevated, their elevation would also predict many more BVR anomalies than actually occurred if there were a causative relation. Additionally, the 2004–2006 period is our worst case charging period yet no BVR anomalies occurred across the POES spacecraft.

The participation of a multidisciplinary anomaly response team is needed in order to confirm or rule out a suspected space environmental root cause [18]. Initially attractive space environmental causes have subsequently been ruled out based on a complete engineering assessment [19]. The longer the series of anomalies, the more likely coincidences can be either ruled out as due to chance or confirmed as identifying root cause [20]. In the present case, the anomaly response team included space environmental expertise early on and identified IC as a possible root cause. With the benefit of a longer time series of anomalies and the analysis method described in this paper, IC now appears to be an unlikely root cause in the absence of an additional, enabling physical mechanism.

V. Conclusion

We have created new estimates of ~MeV electron charge accumulation for highly inclined LEO orbits for ~17.5 years, from 1998 to 2015. We have used these estimates to assess the likelihood that the space environment and deep charging caused a series of power system anomalies on orbit. Overall, the BVR anomalies are not well correlated with IC estimates for any of the standard dielectric charge dissipation time constants used in this paper, and a definitive connection between these anomalies and IC/IESD from >300 and >800 keV electrons cannot be established.

Acknowledgment

The authors would like to thank D. Evans (NOAA/SWPC retired), J. Mazur, and T. Guild (Aerospace Corp) for informative discussions. Software, documentation and data files used in this paper are available from the NCEI POES and Metop satellite service ([6], [36]; http://www.ngdc.noaa.gov/stp/satellite/poes).

References

[1] NOAA Satellite and Information Service: Office of Systems Development (OSD). (2008). *NOAA N-Prime Instrument Description*, accessed on Feb. 29, 2016. [Online]. Available: http://www.osd.noaa.gov/Spacecraft%20Systems/Pollar_Orbiting_Sat/NOAA_N_Prime/POES_N-Prime_9-26-08.doc

[2] NOAA Office of Satellite and Product Operations. *NOAA18 EPS Subsystem Summary*, accessed on Feb. 29, 2016. [Online]. Available: http://www.ospo.noaa.gov/Operations/POES/NOAA18/eps.html

[3] NOAA Satellite Information System (NOAASIS). *POLAR Spacecraft Status Reports*, accessed on Feb. 29, 2016. [Online]. Available: http://noaasis.noaa.gov/NOAASIS/ml/podocs/?C=M;O=A

[4] P. O'Brien *et al.*, "Recommendations for contents of anomaly database for correlation with space weather phenomena," Aeros. Corp., El Segundo, CA, USA, Tech. Rep. TOR-2011(3903)-5, Nov. 10, 2011.

[5] P. O'Brien, D. G. Brinkman, J. E. Mazur, J. F. Fennell, and T. B. Guild. (2012). "A human-in-the-loop decision tool for preliminary assessment of the relevance of the space environment to a satellite anomaly," AEROSPACE TOR-2011(8181)-2 Revision A.

[6] R. J. Redmon *et al.*, "Improved polar and geosynchronous satellite data sets available in common data format at the coordinated data analysis web," *Space Weather*, vol. 13, no. 5, pp. 254–256, May 2015, doi: 10.1002/2015SW001176.

[7] J. C. Green. (2013). *TED Data Processing Algorithm Theoretical Basis Document, version 1.0, 81 NOAA National Geophysical Data Center*. [Online]. Available: http://www.ngdc.noaa.gov/stp/satellite/poes/documentation.html

[8] J. C. Green. (2013). *MEPED Telescope Data Processing Algorithm Theoretical Basis Document. Version 1.0, 77, NOAA National Centers for Environmental Information*, accessed on Feb. 29, 2016. [Online]. Available: http://www.ngdc.noaa.gov/stp/satellite/poes/documentation.html

[9] D. S. Evans and M. S. Greer, "Polar orbiting environmental satellite space environment monitor-2: Instrument descriptions and archive data documentation," Space Weather Predict. Cent., Boulder, CO, USA, NOAA Tech. Mem. 93, version 2.0, 2004.

[10] K. Yando, R. M. Millan, J. C. Green, and D. S. Evans, "A Monte Carlo simulation of the NOAA POES medium energy proton and electron detector instrument," *J. Geophys. Res.*, vol. 116, no. A10, p. A10231, Oct. 2011, doi: 10.1029/2011JA016671.

[11] M. Bodeau, "High energy electron climatology that supports deep charging risk assessment in GEO," in *Proc. 48th AIAA Aerosp. Sci. Meeting*, Orlando, FL, USA, Jan. 2010.

[12] J. F. Fennell, J. L. Roeder, and J. B. Blake, "Internal charging hazards in near-earth space: MEO and HEO orbits," Aeros. Corp., El Segundo, CA, USA, Rep. ATR-2012(8942)-4, Aug. 15, 2012.

[13] T. M. Skov, J. F. Fennell, J. L. Roeder, J. B. Blake, and S. G. Claudepierre, "Internal charging hazards in near-earth space during solar cycle 24 maximum: Van allen probes measurements," *IEEE Trans. Plasma Sci.*, vol. 43, no. 9, pp. 3070–3074, Sep. 2015, [Online]. Available: http://doi.org/10.1109/TPS.2015.2468214

[14] C. E. McIlwain, "Coordinates for mapping the distribution of magnetically trapped particles," *J. Geophys. Res.*, vol. 66, no. 11, pp. 3681–3691, Nov. 1961, doi: 10.1029/JZ066i011p03681.

[15] J. Vollmer, Jr., and C. Gliniak, "Power management on POES as a result of solar array shunt degradation," in *Proc. SpaceOps*, 2010. [Online]. Available: http://doi.org/10.2514/6.2010-2127

[16] J. A. Van Allen, D. N. Baker, B. A. Randall, and D. D. Sentman, "The magnetosphere of Jupiter as observed with Pioneer 10: 1. Instrument and principal findings," *J. Geophys. Res.*, vol. 79, no. 25, pp. 3559–3577, 1974, doi: 10.1029/JA079i025p03559

[17] R. S. Selesnick and J. B. Blake, "On the source location of radiation belt relativistic electrons," *J. Geophys. Res.*, vol. 105, no. A2, pp. 2607–2624, Feb. 2000, doi: 10.1029/1999JA900445

[18] J. Mazur, T. Guild, and P. O'Brien, "The anomaly investigation process," presented at the Spacecraft Anomalies Failures Workshop, Chantilly, VA, USA, Oct. 2015.

[19] M. Bodeau, "Killer electrons from the angry Sun did not stop the pagers," *Space Weather*, vol. 5, no. 3, p. S03006, Mar. 2007, doi: 10.1029/.2006SW000266

[20] J. E. Mazur, J. F. Fennell, J. L. Roeder, P. T. O'Brien, T. B. Guild, and J. J. Likar, "The timescale of surface-charging events," *IEEE Trans. Plasma Sci.*, vol. 40, no. 2, pp. 237–245, Feb. 2012.

[21] S. Agostinelli *et al.*, "Geant4—A simulation toolkit," *Nucl. Instrum. Methods Phys. Res. A Accel., Spectrometers, Detectors Assoc. Equip.*, vol. 506, no. 3, pp. 250–303, Jul. 2003.

[22] J. Allison *et al.*, "Geant4 developments and applications," *IEEE Trans. Nucl. Sci.*, vol. 53, no. 1, pp. 270–278, Feb. 2006.

[23] J. Bartels, "Twenty-seven day recurrences in terrestrial-magnetic and solar activity, 1923–1933," *Terr. Magn. Atmos. Electr.*, vol. 39, no. 3, pp. 201–202a, 1934, doi: 10.1029/TE039i003p00201.

[24] M. Sugiura, "Hourly values of equatorial Dst for the IGY," *Ann. Int. Geophys*, vol. 35, pp. 7–45, Jan. 1964.

[25] N. P. Meredith, R. B. Horne, J. D. Isles, and J. C. Green, "Extreme energetic electron fluxes in low Earth orbit: Analysis of POES E > 30, E > 100, and E > 300 keV electrons," *Space Weather*, vol. 14, no. 2, pp. 136–150, Feb. 2016. [Online]. Available: http://doi.org/10.1002/2015SW001348

[26] D. C. Ferguson, W. Denig, and J. V. Rodriguez, "Plasma conditions during the Galaxy 15 anomaly and the possibility of ESD from subsurface charging," presented at the 49th AIAA Aeros. Sci. Meeting including New Horizons Forum Aeros. Expo., Orlando, FL, USA, Sep. 2011.

[27] T. M. Loto'aniu *et al.*, "Space weather conditions during the Galaxy 15 spacecraft anomaly," *Space Weather*, vol. 13, no. 8, pp. 484–502, Aug. 2015. [Online]. Available: http://doi.org/10.1002/2015SW001239

[28] H. B. Garrett, "The charging of spacecraft surfaces," *Rev. Geophys. Space Phys.*, vol. 19, no. 4, pp. 577–616, Nov. 1981, doi: 10.1029/RG019i004p00577

[29] A. Whittlesey and H. B. Garrett, "NASA's technical handbook for avoiding on-orbit ESD anomalies due to internal charging effects," in *Proc. 6th Spacecraft Charging Technol. Conf.*, AFRL-VS-TR-20001578, Sep. 1, 2000.

[30] J. F. Fennell, H. C. Koons, J. L. Roeder, and J. B. Blake, "Spacecraft charging: Observations and relationship to satellite anomalies," in *Proc. 7th Spacecraft Charging Technol. Conf.*, 2001, pp. 279–285.

[31] P. C. Anderson, "Characteristics of spacecraft charging in low Earth orbit," *J. Geophys. Res.*, vol. 117, no. A7, p. A07308, Jul. 2012, [Online]. Available: http://doi.org/10.1029/2011JA016875

[32] *Mitigating In-Space Charging Effects—A Guideline*, document NASA-HDBK-4002A, NASA, Washington, DC, USA, 2011.

[33] J. H. Adams, "Cosmic ray effects on microelectronics, part IV," NRL Memorandum Rep. 5901, Dec. 31, 1986. [Online]. Available: www.dtic.mil/cgi-bin/GetTRDoc?AD=ADA176611

[34] J. J. Likar, A. L. Bogorad, R. E. Lombardi, S. E. Stone, and R. Herschitz, "On-orbit SEU rates of UC1864 PWM: Comparison of ground based rate calculations and observed performance," *IEEE Trans. Nucl. Sci.*, vol. 59, no. 6, pp. 3148–3153, Dec. 2012. [Online]. Available: http://doi.org/10.1109/TNS.2012.2224128

[35] S. L. Koontz *et al.*, "Materials interactions with space environment: International space station—May 2000 to May 2002," in *Protection of Materials and Structures From Space Environment*, vol. 5, J. I. Kleiman and Z. Iskanderova, Eds. Dordrecht, The Netherlands: Springer, 2004.

[36] *POES Space Environment Monitor, Energetic Particles*, Nat. Ocean. Atmos. Admin., Nat. Centers Environ. Inf., NOAA, 1978, doi: 10.7289/V5JS9NC6.

[37] A. L. Vampola, "Thick dielectric charging on high-altitude spacecraft," *J. Electrostatics*, vol. 20, no. 1, pp. 21–30, Oct. 1987.

[38] G. L. Wrenn, "Conclusive evidence for internal dielectric charging anomalies on geosynchronous communications spacecraft," *J. Spacecraft Rockets*, vol. 32, no. 3, pp. 514–520, 1995.

[39] D. Wade, D. Hoffer, and R. Gubby, "Space weather: A space insurer's perspective," presented at the NOAA Space Weather Workshop, Space Weather Impacts, Insurance Ind. Perspective, vol. 9. Boulder, CO, USA, Apr. 2014, accessed on Jul. 25, 2016. [Online]. Available: ftp://ftp.ngdc.noaa.gov/STP/publications/sam/SAM_Hoffer.pdf

[40] R. J. Redmon, J. V. Rodriguez, C. Gliniak, and W. F. Denig, "Internal charge estimates for satellites in LEO and system impacts," in *Proc. 14th Spacecraft Charging Technol. Conf.*, Noordwijk, The Netherlands, 2016.

Robert J. Redmon received the D.B.S. degrees in electrical engineering and computational mathematics from the University of California at Riverside, Riverside, CA, USA, in 1998, the M.S. degree in electrical engineering from the University of Notre Dame, Notre Dame, IN, USA, in 2000, and the Ph.D. degree in aerospace engineering sciences from the University of Colorado Boulder, Boulder, CO, USA, in 2012.

He joined the Solar and Terrestrial Physics Division within NOAA's National Centers for Environmental Information (NCEI), as a Physical Scientist, in 2003. His professional activities have included developing radar systems for ionospheric sounding, facilitating information exchange through the world data service, studying auroral processes, and magnetic fields at LEO and GEO, calibrating space-borne magnetometers, and investigating satellite anomalies.

Dr. Redmon received the Goodrich Aerostructures Engineering Scholarship from 1993 to 1998, and held a University of Notre Dame Arthur J. Schmitt Leadership Fellowship from 1998 to 2000.

Juan V. Rodriguez received the B.S., M.S., and Ph.D. degrees in electrical engineering from Stanford University, Stanford, CA, USA, in 1987, 1988, and 1994, respectively.

He joined the Cooperative Institute for Research in Environmental Sciences (CIRES), University of Colorado Boulder, Boulder, CO, USA, in 2009, where he is currently a Senior Research Scientist working within the NOAA National Centers for Environmental Information (NCEI). His professional activities have included research on optical and plasma signatures of polar cap, dayside and pulsating aurora, on the cross-calibration of satellite charged particle measurements, and on the access of solar energetic particles inside Earth's magnetosphere. His applied work has included spacecraft anomaly investigations and the development of algorithms for processing and re-processing GOES particle measurements.

Dr. Rodriguez held a National Science Foundation Graduate Fellowship from 1988 to 1991, a National Aeronautics and Space Administration Graduate Student Researchers Program Fellowship from 1991 to 1994, and a National Research Council / Air Force Office of Scientific Research Research Associateship from 1994 to 1996.

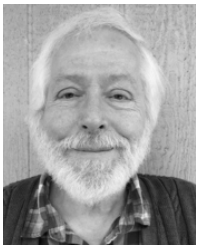

Carl Gliniak received the B.S. degree in physics from the University of Massachusetts, Lowell, MA, USA, the M.S. degree in solid-state physics with the completion of all Ph.D. coursework from Northeastern University, Boston, MA, USA, and the M.S. degree in optical signal and information processing from the School of Electrical Engineering, Georgia Institute of Technology, Atlanta, GA, USA.

He has over 30 years of experience in aerospace engineering. He has numerous publications, several of which are company proprietary. He has worked on government contracts for DOD, NASA, and NOAA that encompassed pre-Phase A (new missions/development) through Phase F (satellite mission decommissioning/disposal) for mission engineering support. He was with the NOAA NESDIS Satellite Operations Control Center for the past 15 years, as a Contractor and later with the Government. While at NSOF (NOAA Satellite Operations Facility), he was responsible for the POES, Jason, and Metop missions. He is currently the acting POES/Jason/Metop Team Lead, spacecraft bus and payload lead, and has been the Ground System Engineer for the above missions.

Mr. Gliniak is a former member of the IEEE, the OSA, and the SPIE professional societies.

William F. Denig received the Ph.D. degree from Utah State University, Logan, UT, USA, in 1983.

Before joining NOAA in 2005, he spent 22 years with the Air Force Research Laboratory, Hanscom Air Force Base, MA, USA, where he was the Chief of the Space Weather Center of Excellence and the Deputy Chief Scientist. He was temporarily assigned to the Air Force Space Command in Colorado Springs, CO, USA, and the National Operational Environmental Satellite System Program Office in Silver Spring, MD, USA. As a participant of the Air Force's Windows on Europe Program, he was a Visiting Scientist with the Physics Department of the University of Oslo, Oslo, Norway. At NOAA, he was the Chief of the Solar and Terrestrial Physics Division and Director of the World Data Center for Solar-Terrestrial Physics. He is currently a Supervisory Physical Scientist within the NOAA National Centers for Environmental Information.